INTERNATIONAL JOURNAL OF AUTOMOTIVE AND MECHANICAL ENGINEERING
ISSN: 2229-8649 e-ISSN: 2180-1606
VOLUME 22, ISSUE 4, 2025, 13104 - 13116
DOI: https://doi.org/10.15282/ijame.22.4.2025.20.0997

RESEARCH ARTICLE

Crystalline Nanocellulose as a Potential Alternative to Metallic Nanofuel Additives: An Experimental Investigation

Kerem Keskin, Abdülvahap Çakmak*

Faculty of Engineering and Natural Sciences, Department of Mechanical Engineering, Samsun University, Samsun, 55420, Türkiye

ABSTRACT – Crystalline nanocellulose (CNC), derived from various biomass sources, is gaining attention as a sustainable nanomaterial for energy applications due to its high surface area-to-volume ratio, lightweight nature, biodegradability, and associated environmental benefits. This experimental research investigated the potential of CNC as an alternative to traditional metallic nanofuel additives, presenting preliminary results that have not been previously reported. Commercially available CNC was blended into standard diesel fuel at concentrations of 100 ppm, 250 ppm, and 500 ppm, and engine performance and emission tests were conducted. CNC demonstrated potential as a nanofuel additive in diesel, offering benefits like improved combustion, enhanced engine performance, and reduced NOx emissions and exhaust smoke opacity. However, higher concentrations were less effective in lowering nitrogen oxides (NOx) levels, and carbon dioxide (CO_2) emissions increased due to more complete combustion. The highest engine performance was achieved with a CNC concentration of 500 ppm, resulting in an average reduction in brake-specific fuel consumption (BSFC) by 3.95% and an increase in brake thermal efficiency (BTE) by 2.73% compared to diesel fuel. The fuel cost analysis indicated that CNC is economically viable at a 100-ppm concentration; however, higher concentrations resulted in a substantial increase in fuel costs, despite reducing fuel consumption. The initial results are promising and suggest CNC could be a suitable alternative to traditional metallic nanofuel additives.

ARTICLE HISTORY
Received : 27th Apr. 2025
Revised : 25th Aug. 2025
Accepted : 29th Nov. 2025
Published : 21st Dec. 2025

KEYWORDS
Crystalline nanocellulose
Diesel engine
Engine performance
Fuel additive
Nanofuel

1. INTRODUCTION

Internal combustion engines (ICEs) degrade the environment by emitting pollutants during the combustion of fossil fuels. Reducing greenhouse gas emissions in transportation requires adopting electrification and renewable fuels [1]. While transportation is shifting toward electrification, heavy-duty transport will still depend on ICEs and traditional fuels for decades to come, just as it has until now [2]. Advancements in engine technology and emissions control systems have made internal combustion engines more efficient and cleaner [3]. However, further improvements are needed to address energy and environmental challenges. Ongoing advancements include combustion technologies, hydrogen engines, biofuels, and synthetic fuels [4]. However, these innovations are still in their early stages and have not yet achieved widespread real-world adoption. A more practical and cost-effective approach is to use fuel additives, which offer several benefits, particularly in enhancing the performance and efficiency of internal combustion engines while reducing environmental impact [5].

Several fuel additives have been used to enhance fuel quality, improve combustion, reduce emissions, and extend engine durability [6]. However, in recent decades, nanoparticles have emerged as promising additives for conventional and biofuels in engines [7]. Therefore, nanoparticles are being increasingly explored as fuel additives due to their unique properties, including a high surface area-to-volume ratio, exceptional catalytic activity, enhanced thermal conductivity, and multifunctionality [8]. Many studies have explored the effects of metal-based nanoparticles, including alumina (Al_2O_3), cerium oxide (CeO_2), titanium dioxide (TiO_2), iron oxide (Fe_2O_3), copper oxide (CuO), zinc oxide (ZnO), magnesium oxide (MgO), manganese oxide (MnO_2), nickel oxide (NiO), and silicon oxide (SiO_2) on internal combustion engines. These studies [9-13] have concluded that adding metallic nanoparticles to base fuels can enhance their thermophysical properties, including kinematic viscosity, density, distillation characteristics, and cetane number. Due to their catalytic effect, nanoparticles can also enhance combustion by reducing ignition delay and increasing the combustion rate. Furthermore, nanoparticle additives have been demonstrated to enhance thermal efficiency and power output while reducing fuel consumption and carbon emissions in diesel engines.

Although metallic nanoparticles are widely accessible and sold commercially, their high cost and significant toxicity often overshadow their advantages. As a result, green synthesis methods for metallic nanoparticles have gained increasing importance in recent years, leading several studies to focus on this approach. For example, in the experimental study by Doğan et al. [14], SiO_2 and TiO_2 nanoparticles produced via green methods were added to diesel–biodiesel blends at various concentrations. These nanofuels were then tested in a diesel engine to evaluate their impact on engine operation. The results obtained were promising; however, the study emphasized that further research is needed to fully understand the potential and long-term impacts of green-synthesized metallic nanoparticles in fuel applications. Moreover, carbon-

*CORRESPONDING AUTHOR | A. Çakmak | ✉ abdulvahap.cakmak@samsun.edu.tr

based nanoparticles, such as carbon nanotubes, graphene, and graphite, have been researched as potential nanofuel additives with milder side effects than their metallic counterparts [15]. Despite their potential for improving engine performance and reducing emissions, their main challenges are high production costs, low product yield, and concerns about toxicity [16]. Metallic nanoparticles contribute to engine metallic emissions, resulting in additional environmental impacts and risks to human health [17]. Consequently, the installation of new nanometal trapping systems in the exhaust line is required. These factors explain why carbon-based and metallic nanofuel additives have not yet been commercially used as fuel additives. Therefore, researching nanofuel additives made from abundant natural raw materials that are easy to produce and have no toxic effects is essential.

The background above raises the question of whether non-toxic, naturally derived nanocellulose can serve as a nanofuel additive. Cellulose is one of the most abundant natural substances and a sustainable resource [18]. Nanocellulose is a renewable, eco-friendly material that is easy to produce at a low cost and with high yield. A comparison framework of CNC versus metallic nanoparticles as nanofuel additives is presented in Table 1. Given these properties, it can be a nanofuel additive alternative to metallic nanoparticles.

Table 1. A comparison framework of CNC versus metallic nanoparticles

Specification	CNC	Metallic Nanoparticles (e.g., CuO, TiO, Al_2O_3)
Source	Biomass	Mineral based
Renewability	Renewable	Non-renewable
Biodegradability	Biodegradable	Non-biodegradable
Toxicity	Low	Toxic or carcinogenic
Environmental impact	Low	High: Accumulate in the environment
Cost	Relatively low	Often expensive
Stability in fuel	Stable for two hours*	Mostly unstable and requires stabilizers
Thermal Conductivity	Moderate	High
Production method	Acid hydrolysis or a mechanical process	Sol-Gel Process, Electrochemical Etching, Laser Ablation, Co-precipitation

*Observed in this experimental study

When cellulose, a plant-based polymer, is broken into nano-sized pieces via mechanical or chemical processes, nanocellulose is formed and applied in various technologies. It is a novel nanomaterial with crystalline or fibrous structures, diameters ranging from 5 to 500 nm, and varying lengths. Nanocellulose, produced by reducing cellulose to the nanoscale, is classified based on size, properties, and production methods. Microfibrillated cellulose results from the mechanical breakdown of wood pulp, while nanocrystalline cellulose is obtained through acid hydrolysis. Crystalline nanocellulose (CNC) consists of nano-sized cellulose fibrils in crystalline form. These submicroscopic particles possess various properties, including high strength, electromagnetic responsiveness, and a large surface area. CNC has a wide range of applications across various fields. In this study, CNC was preferred due to its suitable dimensions, specifically 10–20 nm in diameter and 300–900 nm in length. CNC has the potential to replace metal nanofuel additives. However, to the authors' knowledge, no previous studies have explored the use of nanocellulose as a fuel additive in engine applications. Therefore, this study aims to evaluate CNC's potential as a nanofuel additive. To achieve this, commercially available CNC was dispersed into conventional diesel fuel at concentrations of 100 ppm, 250 ppm, and 500 ppm by applying mechanical and ultrasonic homogenization without the use of surfactants. Some fuel properties were analyzed, followed by engine tests. The findings contribute to filling the existing research gap and provide a foundation for further studies.

2. METHODS AND MATERIALS

CNC, with a diameter of 10–20 nm and a length of 300–900 nm, was supplied from Nanografi. Table 2 lists its specifications. Its morphology and chemical composition were analyzed using a JEOL JSM-7001F scanning electron microscope (SEM) and energy-dispersive X-ray (EDX) spectroscopy. Figure 1 presents SEM images of CNC at 5k magnification (left) and 10k magnification (right). The CNC particles exhibit an irregular, aggregated morphology, forming clustered structures. Smaller particles adhere to larger ones, indicating aggregation. At 10k magnification, some structures appear smooth with a rounded or capsule-like shape, likely due to the acid hydrolysis production process. Moreover, the high magnification image (10k) highlights finer details, revealing surface textures and possible porosity. Figure 2 displays the CNC EDX spectrum. EDX analysis reveals the overall elemental composition with an error margin of approximately 10%. This analysis indicates that CNC primarily consists of carbon (57.3% wt), oxygen (39.7% wt), and sulfur (1.2% wt).

Table 2. Technical properties of the CNC [19], [20]

Specification	
Color	White
Form	Dry powder ($\sim\%4\ wt.moisture$)
Average Particle Size	10-20 nm wide and 300-900 nm length
Cellulose Crystallinity (XRD)	92%
Decomposition Temperature (TGA in N2)	349 ℃
Density/Bulk Density	1.49 g/cm^3/0.5-0.8 g/cm^3
Surface area	~ 200 m^2/g

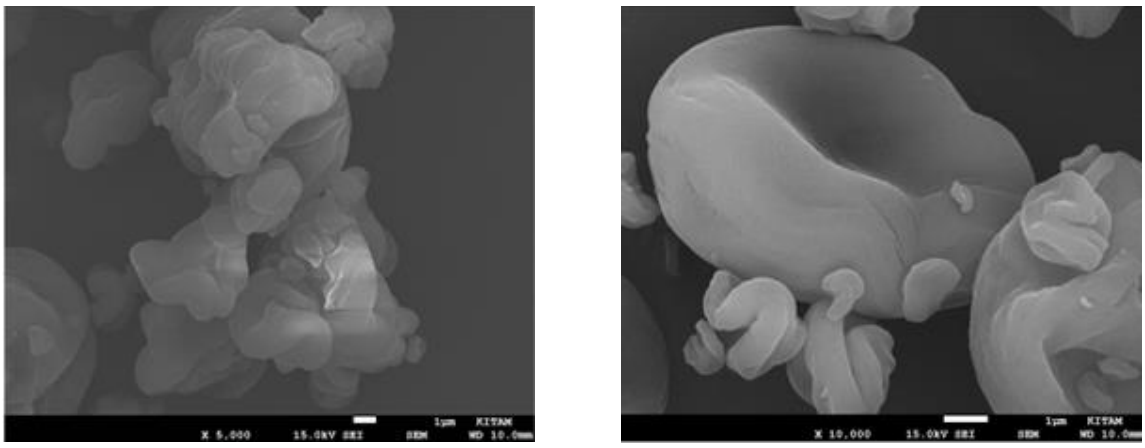

(a) (b)

Figure 1. SEM images of CNC at (a) 5k magnification; (b) 10k magnification

Figure 2. EDX spectrum of CNC

The next step in experimentation was preparing the nanofuels. CNC was dispersed in diesel fuel at concentrations of 100 ppm, 250 ppm, and 500 ppm. CNC is expected to increase fuel viscosity, so its maximum concentration was restricted to 500 ppm. In the nanofuel preparation stage, no surfactant was used to prevent potential interference with engine test results. Homogeneity of the nanofuel was achieved through a two-step process involving mechanical and ultrasonic mixing. First, the blend was stirred with a magnetic stirrer at 1500 rpm for 15 minutes. Then, an ultrasonic probe (SONIC Vibra cell^{TM}) operating at 40 kHz and 750W was used for 15 minutes to further enhance dispersion. This process ensured the uniform distribution of CNC in the fuel. A schematic illustration of the stages for preparing test fuels is shown in Figure 3. Diesel fuel (DF) without CNC was used as a baseline for comparison. Due to the white color of CNC, no naked-eye visible color changes occurred in nanofuels. Nanofuels remained stable for two hours, with no visible coagulation or sedimentation observed upon inspecting the fuel samples at the end of this period, as shown in Figure 4.

Various fuel properties were measured by following related standards, including density (EN ISO 12185), flash point (EN ISO 2719), cold filter plugging point (EN 116), and distillation temperatures (EN ISO 3405). The measurement results are provided in Table 3. Figure 5 illustrates the engine test setup. The test engine (1) is a four-stroke, water-cooled, direct injection diesel engine with a displacement of 665 cm³ and a rated brake power of 3.5 kW. The engine's torque was

measured using an Eddy-current dynamometer [(2)]. The control unit [(3)] regulates engine load and coolant flow rate while displaying all relevant temperature and flow measurements. It also includes the charge amplifier and data acquisition card. Cylinder pressure was measured over 100 cycles, and the average data were processed for combustion analysis. An emission measurement unit [(4)], comprising the Test-350XL gas analyzer and Bosch BEA 070 smoke meter, was used to assess gaseous emissions and exhaust gas smoke opacity. The gas analyzer can detect O_2, NO_X, CO, and CO_2 in the exhaust stream with accuracies of ±0.8%, ±10 ppm, ±5 ppm, and ±0.2%, respectively. The smoke meter has a measuring range of 0-100% with an accuracy of ±1%. A fuel flow meter [(6)] measured the fuel volumetric flow rate. Separate fuel tanks [(7), (8)] allowed the engine to be fueled independently. The electrical panel [(9)] serves as a control center for distributing electricity to the test setup.

The test engine was operated with its original configuration, which included a compression ratio of 17.5/1, a fuel injection pressure of 20 MPa, and a fuel injection advance of 23 crank angles (°CA). At the start of the engine test, the engine was warmed up for 30 minutes to ensure the coolant temperature remained stable between 333 K and 338 K. After warming up, the engine was operated with each test fuel. Engine tests were conducted at 0%, 25%, 50%, 75%, and 100% of the engine's rated power output, with the engine speed maintained at 1500 rpm throughout all experiments. The selected engine loadings also correspond to brake mean effective pressure (BMEP) of 0.0 MPa (idle), 0.1 MPa, 0.2 MPa, 0.3 MPa, and 0.4 MPa, respectively.

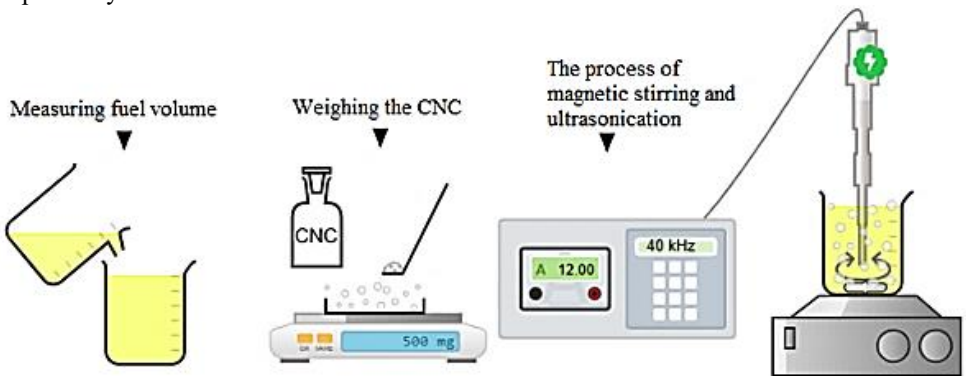

Figure 3. Schematic illustration of the stages for preparing nanofuels

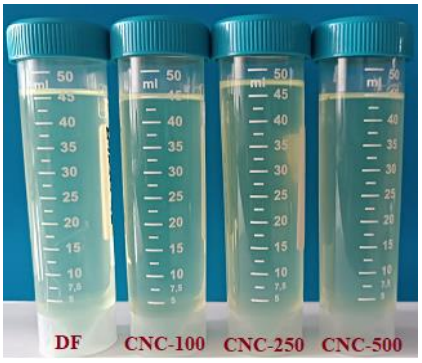

Figure 4. Actual image of diesel fuel and nanofuel samples at the end of the two hours

Table 3. Specification of the test fuels

	Property	EN 590 limit	DF*	CNC-100 ppm	CNC-250 ppm	CNC-500 ppm
	Density @15 ℃, kg/m^3	820-845*	832.9	832.9	833.1	833.2
	Flashpoint, ℃	min. 55	61.0	62.0	63.0	64.0
	CFPP,℃	max. 5	-7	-7	-7	-7
Distillation, °C	Initial boiling p.	-	153.3	158.0	162.3	161.0
	T10	-	205.5	207.6	206.9	207.4
	T50	-	271.2	271.9	271.8	271.8
	T90	-	338.5	339.9	340.0	339.2
	Final boiling p.	-	362.6	363.2	362.5	363.0
	250 ℃, % (v/v)	max. 65	35.9	35.6	35.8	35.5
	350 ℃, % (v/v)	min. 85	94.4	94.1	94.2	94.2
	%95 (v/v), ℃	max. 360	352.3	353.3	352.8	352.7

*Type A (summer diesel fuel), Sales range: April 1 - October 31 (±15 days)

For each test fuel and operating condition, four measurements were recorded for performance parameters, including engine torque, engine speed, fuel flow rate, intake air flow rate, engine coolant flow rate, and exhaust gas temperature. The average of four readings was then used for performance evaluation. Similarly, six measurements were recorded for each emission parameter, and the average value was used for comparative analysis. This approach minimizes measurement errors and enhances the reliability of the results. However, uncertainty analysis is necessary to demonstrate the accuracy of the measurements quantitatively. The method proposed by Holman [21] was employed to determine the uncertainties associated with the calculated parameters. The uncertainties for brake power, fuel consumption, brake specific fuel consumption (BSFC), and brake thermal efficiency (BTE) were computed as 0.4655%, 0.6876%, 0.8303%, and 0.8199%, respectively. The exhaust emission analyzers were calibrated before the experiments and verified for accurate functioning and measurement reliability.

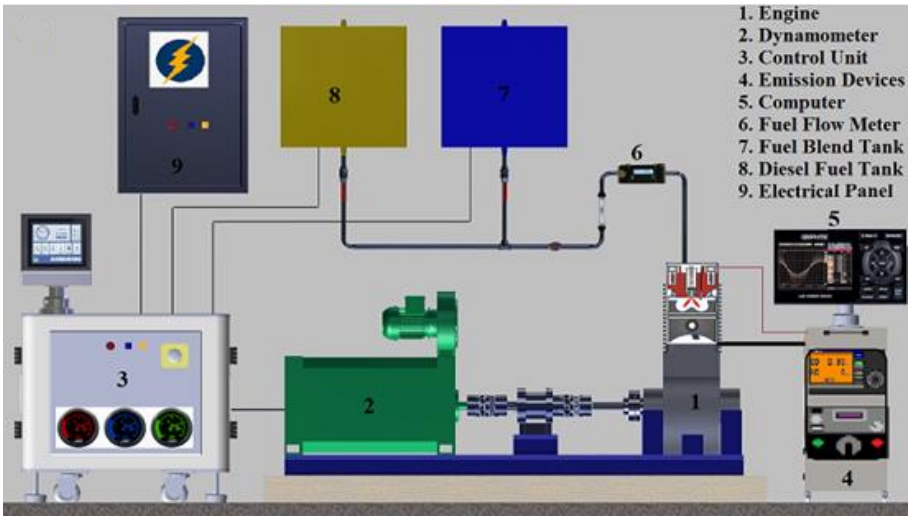

(a)

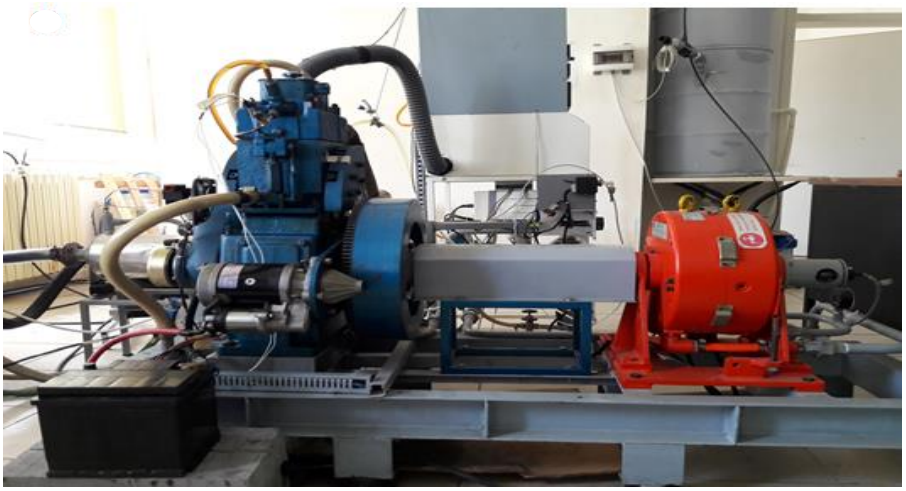

(b)

Figure 5. Schematic representation (a) and actual photograph (b) of the engine test setup

Fuel cost analysis is crucial for optimizing fuel usage, ensuring economic feasibility, and informing the adoption of more efficient or sustainable energy solutions. It has been noted that most studies in the literature regarding the application of nanofuel additives in engines lack a comprehensive cost analysis. In the few studies [22]–[24] that do address cost, the focus is typically limited to the increase in fuel price per liter resulting from the addition of nanoparticles. However, nanoparticles raise the per-liter fuel cost and reduce the engine's fuel consumption. Therefore, a more accurate and meaningful cost assessment should consider both the increased fuel cost and the improved fuel efficiency. In this study, a cost analysis was performed by considering both fuel price and brake-specific fuel consumption. For this analysis, the equation given below was utilized:

$$F_{cost} = BSFC \times P_{fuel} \times \rho^{-1} \quad (€/kWh) \tag{1}$$

where BSFC is the brake-specific fuel consumption (kg/kWh), P_{fuel} $(€/L)$ is the fuel price per liter, and ρ (kg/L) is the fuel density. In Türkiye, as of September 2024, the prices of diesel fuel and CNC were 1.15 €/L and 4.86 €/g, respectively. The price of CNC-100 ppm, CNC-250 ppm, and CNC-500 ppm fuels was computed as 1.63 €/L, 2.36 €/L, and 3.58 €/L, respectively.

3. RESULTS AND DISCUSSION

As shown in Table 3, the addition of CNC up to the concentration of 500 ppm slightly affected the measured fuel properties. It led to an increase in fuel density, flash point temperature, and distillation temperatures. However, the fuel's cold filter plugging point (CFPP) remained unaffected by the inclusion of CNC. Among the tested fuels, CNC-500 showed the highest density and flash point, with increases of 0.300 kg/m³ and 3 °C, respectively, compared to the base diesel. These improvements are beneficial because higher density boosts volumetric energy content, and a higher flash point enhances safety during storage and handling. Regarding the measured fuel properties, all test fuels met the EN590 diesel specification, confirming their suitability for practical use and compatibility with existing diesel engines and fuel infrastructure.

Figure 6 shows the in-cylinder pressure changes of the test fuels at full load and 1500 rpm. The peak cylinder pressures recorded were 61.44 bar for DF, 59.82 bar for CNC-100 ppm, 60.92 bar for CNC-250 ppm, and 62.02 bar for CNC-500 ppm. The addition of CNC had a slight influence on the combustion and cylinder pressure characteristics. At a lower concentration (100 ppm), CNC caused a minor decrease in premixed combustion intensity, resulting in lower cylinder pressure compared to diesel. At this level, CNC may not yet achieve sufficient fuel-air homogenization or a catalytic effect to improve combustion significantly. Increasing the CNC dose to 250 ppm partially offset these effects, producing a pressure profile closer to that of DF. The most notable improvement was observed with the 500 ppm blend, which exhibited an earlier rise in pressure, a steeper pressure gradient near top dead centre, and the highest peak pressure among all fuels. This pattern suggests better atomisation, improved fuel–air mixing, and stronger premixed combustion driven by the nanostructure of CNC. Overall, the CNC-500 ppm blend exhibited the most effective combustion characteristics, while lower doses resulted in more moderate changes in the in-cylinder pressure profile.

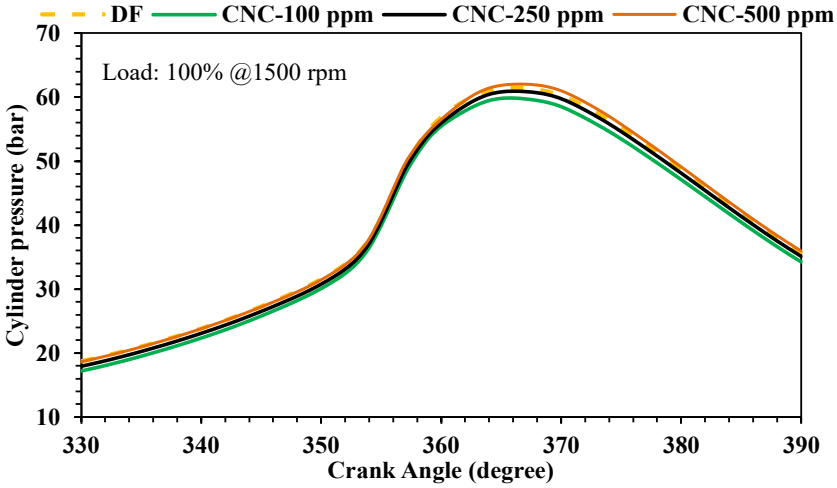

Figure 6. Cylinder Pressure profile for the test fuels at the maximum BMEP test point

The instantaneous heat release was calculated by processing the measured cylinder pressure–crank angle data based on the first law of thermodynamics. This parameter provides valuable insight into the combustion process occurring within the cylinder. Figure 7 presents the net heat release rate (NHRR) profile for the test fuels at the maximum BMEP condition. The NHRR curves indicate that all tested fuels underwent similar premixed and diffusion combustion phases. However, the fuels containing CNC exhibited higher NHRR compared to DF. The peak NHRR values for DF, CNC-100 ppm, CNC-250 ppm, and CNC-500 ppm were 43.06, 43.28, 44.12, and 44.34 J/°CA, respectively, all occurring at a crank angle of 354 °CA. CNC possesses a high surface area and nanoscale structure, which can enhance fuel atomization. This finer fuel spray promotes better evaporation and mixing in the combustion chamber, leading to more efficient combustion and a higher NHRR. Moreover, CNC's structural properties may also contribute to improved combustion stability and a more uniform burn. This can result in a more rapid heat release throughout the combustion cycle, contributing to peak NHRR values. Nanofuel additives may also reduce the ignition delay. Reduced ignition delay in nanofuels results from the combined effects of improved heat transfer, faster droplet evaporation and atomization, catalytic radical formation, oxygen release from nanoparticles, and enhanced air–fuel mixing, all of which speed up the ignition process. The enhanced reactivity of the CNC-fuel mixture can trigger earlier ignition, allowing more fuel to burn during the early stages of the combustion cycle, which leads to a higher NHRR at the same crank angle. However, this effect was not clearly observed in this study, as the difference in ignition delay between the test fuels was negligible. The improvement in the combustion process, achieved through the use of CNC, resulted in enhanced engine performance.

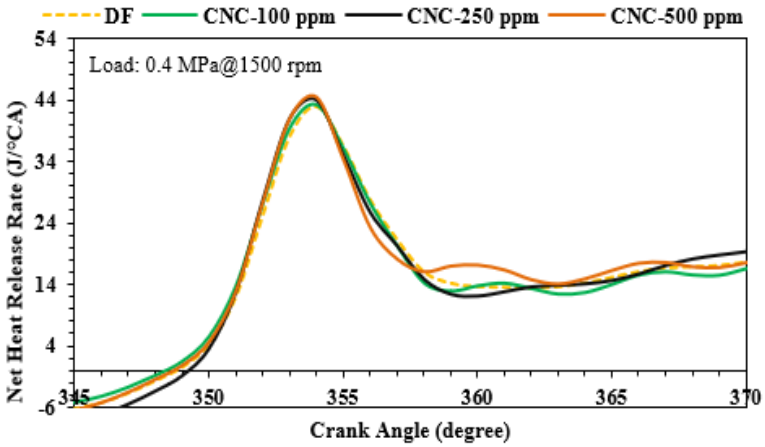

Figure 7. NHRR profile for the test fuels at the maximum BMEP test point

The fuel consumption rate on a mass basis for test fuels across various loadings is presented in Figure 8. The fuel consumption rate increases gradually with engine load to produce the desired power. The effect of CNC on reducing fuel consumption is more pronounced at low, half, and full loads than at full load. Regarding the average fuel consumption rate, adding CNC to DF at concentrations of 100 ppm, 250 ppm, and 500 ppm resulted in decreases of 2.51%, 2.86%, and 4.52%, respectively, compared to DF.

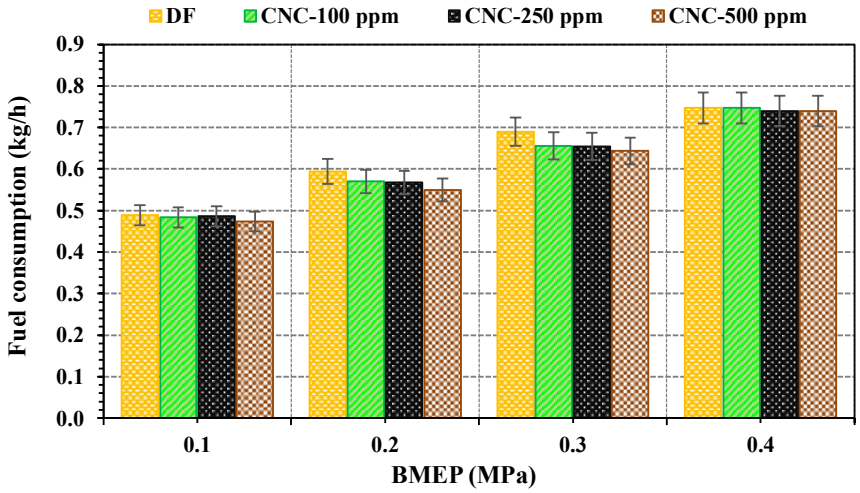

Figure 8. Fuel consumption rate on a mass basis for test fuels across various loadings

For a more meaningful comparison, the BSFC graph is shown in Figure 9. It displays the hourly fuel consumption rate for a power output of one kW. The increase in fuel conversion efficiency as engine load rose resulted in lower fuel consumption for a given power output, thereby decreasing the BSFC. The CNC added fuels that offered enhanced combustion, lowering specific fuel consumption. The CNC-100 ppm, CNC-250 ppm, and CNC-500 ppm nanofuels yielded an average reduction in BSFC by 1.78%, 2.04%, and 3.95%, respectively, compared to DF. The reduction in BSFC when CNC is added to diesel fuel can be attributed to several factors, including enhanced atomization and air-fuel mixing, the catalytic combustion effect, and the oxygenated nature of CNC.

The improvement in BSFC naturally reflects on BTE, as seen in Figure 10. It was observed that the addition of CNC as a fuel additive improved the BTE. Compared to DF, the CNC-100 ppm, CNC-250 ppm, and CNC-500 ppm fuels demonstrated average increases in BTE of 0.66%, 1.26%, and 2.73%, respectively. A more significant improvement in BTE was achieved with increasing CNC concentration. Due to its nanoscale crystalline structure, CNC improves fuel atomization and dispersion in the combustion chamber. Better atomization results in a more homogeneous mixture and, consequently, more effective energy conversion. Furthermore, CNC contains oxygen within its molecular structure, enhancing combustion oxidation reactions. This enables the extraction of more energy from the same amount of fuel, thereby boosting the BTE. These statements align well with the observation of heat release. As mentioned, CNC-containing blends demonstrated higher NHRR, especially in the premixed phase. This allows for more energy to be released, thereby improving efficiency.

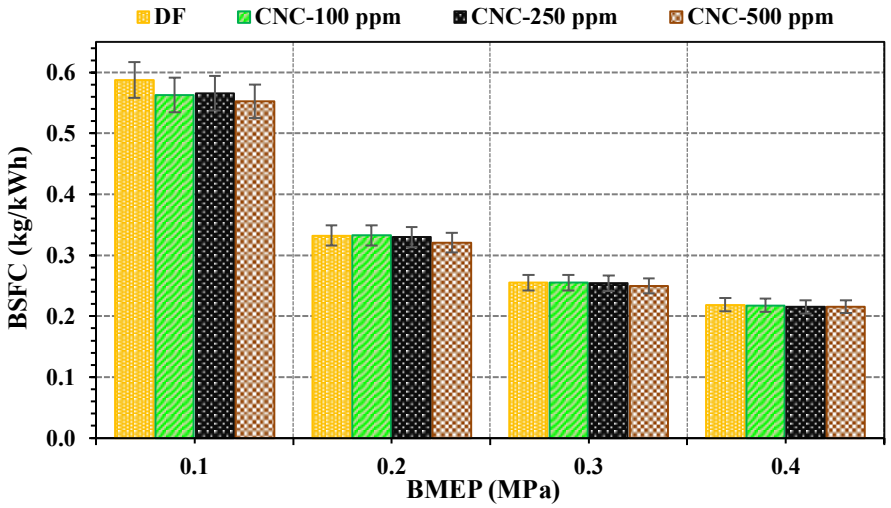

Figure 9. The BSFC for test fuels across various loadings

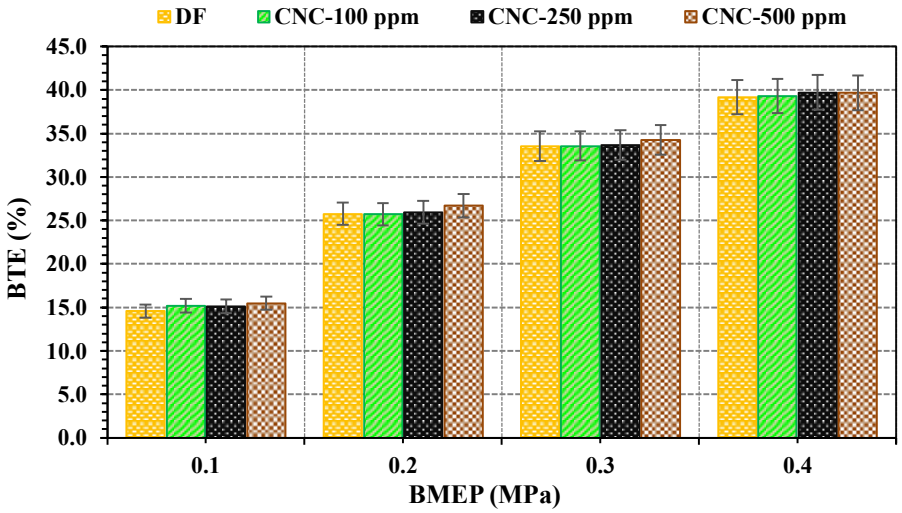

Figure 10. The BTE for test fuels across various loadings

The effect of adding CNC to DF on NOx emissions is presented in Figure 11. NOx emissions primarily form through the thermal NOx mechanism, which is highly sensitive to combustion temperatures and, therefore, increases with rising engine load. When comparing the fuels, DF generally resulted in higher NOx emissions. Although NOx emissions did not show a consistent trend with CNC concentration, the analysis of average values revealed that CNC-100 ppm, CNC-250 ppm, and CNC-500 ppm fuels produced 7.99%, 2.34%, and 3.45% lower NOx emissions, respectively, compared to DF. As CNC concentration increased, combustion efficiency improved, resulting in higher in-cylinder temperatures. This promotes the oxidation of more nitrogen in the cylinder, resulting in increased NOx formation. Therefore, CNC enhanced combustion at higher concentrations to such an extent that its NOx suppression effect diminished. Nevertheless, considering the average NOx levels, all the CNC-added fuels produced lower NOx emissions than DF. Due to its oxygen content, nanostructure, and combustion-modifying effects, CNC functions as both a combustion enhancer and a NOx mitigator, particularly at low-to-moderate concentrations.

The effect of the test fuels on smoke opacity is shown in Figure 12. As engine load increases, fuel injected per cycle increases, resulting in higher smoke opacity. The variation in smoke opacity among the test fuels is not entirely consistent; however, when average values are compared, the CNC-100 ppm, CNC-250 ppm, and CNC-500 ppm fuels exhibited 12.78%, 12.11%, and 13.60% lower opacity, respectively, compared to DF. CNC's nanostructure can enhance the dispersion and spray characteristics of DF, resulting in finer fuel droplets and more homogeneous air–fuel mixing. Additionally, CNC contains chemically bound oxygen, which enhances oxidation reactions during combustion, especially in fuel-rich zones where soot is typically formed. All of these factors contribute to the observable reduction in smoke opacity. The combustible nature of the additive is the most crucial factor in reducing smoke opacity. Unlike metallic nanoparticles, CNC burns completely in the engine cylinder. On the other hand, metallic nanoparticles retain their solid form during combustion and act as nuclei for particulate matter formation by providing surface area for condensing heavy hydrocarbon vapors. Since these particles do not combust, their presence in the exhaust might increase smoke opacity. In contrast, flammable CNC does not contribute to particulate formation, reducing smoke opacity. This makes CNC a viable nano fuel additive.

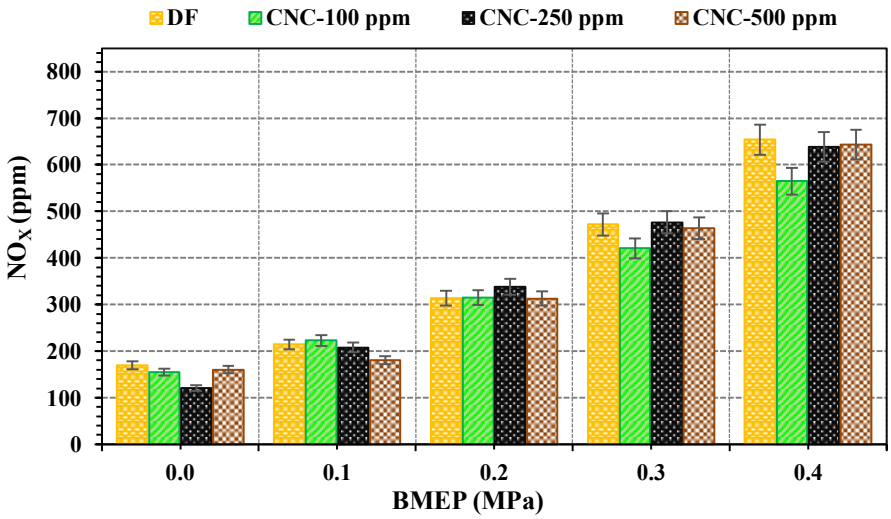

Figure 11. NOx emission for test fuels across various loadings

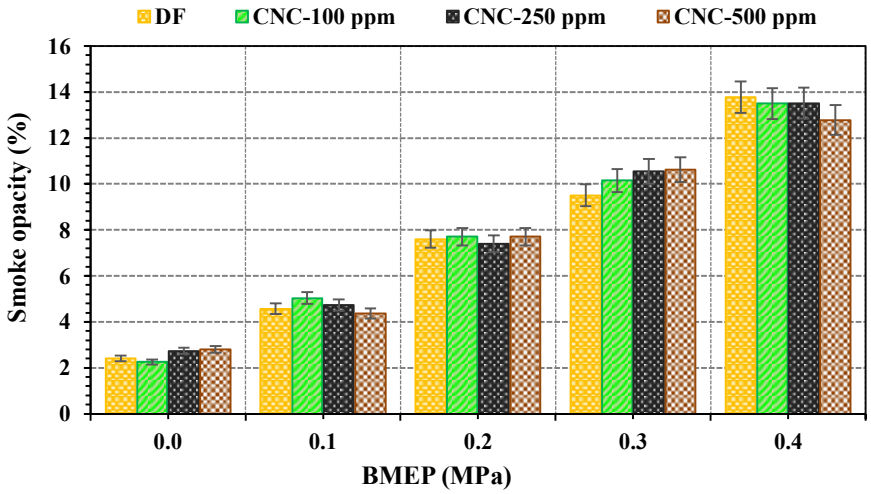

Figure 12. Smoke opacity for test fuels across various loadings

CO_2 emission is a byproduct of the complete combustion of any carbon-containing fuel. Therefore, an increase in CO_2 emissions generally indicates more complete combustion. However, CO_2 emissions can be reduced by lowering specific fuel consumption and utilizing low-carbon or carbon-neutral fuels [25]. Figure 13 presents the measured CO_2 emissions for the test fuels. CO_2 emissions increased with rising engine load due to improved combustion efficiency and higher fuel consumption, reaching their peak at full load. The addition of CNC showed an inconsistent effect on CO_2 emissions, reducing emissions at specific loads while increasing them at others. However, when considering the average CO_2 emission values, the impact of CNC becomes more apparent. Compared to DF, CNC-100 ppm, CNC-250 ppm, and CNC-500 ppm fuels produced, on average, 0.39%, 2.42%, and 2.63% higher CO_2 emissions, respectively. The increase in CO_2 emissions with rising CNC concentration can be attributed to the high surface area-to-volume ratio, which enhances mixture homogeneity and supports more complete combustion. Complete combustion of carbon-containing compounds results in CO_2, rather than partially oxidized products such as CO or unburned hydrocarbons and soot. This explanation is further supported by the observed reduction in smoke opacity for CNC-containing fuels, which suggests a higher degree of combustion completeness.

The fuel cost represents the cost of consumed fuel per hour to generate one kilowatt of brake power output. Figure 14 illustrates the outcomes of the fuel cost analysis. For all test fuels, the cost declined as engine load increased, reaching its lowest point at full engine load. At this operating condition, the fuel costs were recorded as 0.30 €/kWh, 0.31 €/kWh, 0.61 €/kWh, and 0.93 €/kWh for the DF, CNC-100 ppm, CNC-250 ppm, and CNC-500 ppm fuels, respectively. Since fuel cost is directly proportional to BSFC, it exhibited a similar trend to that of BSFC with respect to engine load. Among the tested fuels, CNC-100 ppm demonstrated a fuel cost nearly equivalent to diesel fuel, owing to its reduced BSFC and a unit price only 1.4 times higher than diesel. However, as the CNC concentration increased, the fuel cost rose significantly. This was attributed to the higher unit price of CNC-250 ppm and CNC-500 ppm fuels, which are 2.1 and 3.1 times greater than diesel fuel, respectively, despite their improved BSFC performance. Considering the average fuel cost values, CNC-100 ppm resulted in only a 0.37% increase compared to diesel fuel. In contrast, CNC-250 ppm and CNC-500 ppm fuel increased the fuel cost by 102% and 200%, respectively. These findings suggest that incorporating CNC at a concentration of 100 ppm is a cost-effective approach. However, higher concentrations led to significant

increases in fuel costs that the performance gains could not offset. In this context, the primary driver of fuel cost is the price of CNC, which is nearly 3,500 times higher than diesel fuel on a per-gram basis. Consequently, fuel costs would decrease if the price of CNC were reduced, which could be accomplished through advancements in nanoparticle production technology.

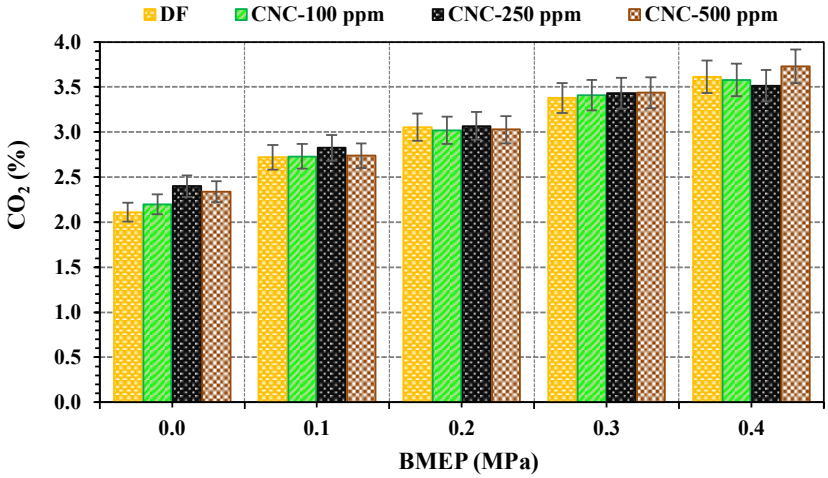

Figure 13. CO_2 emission for test fuels across various loadings

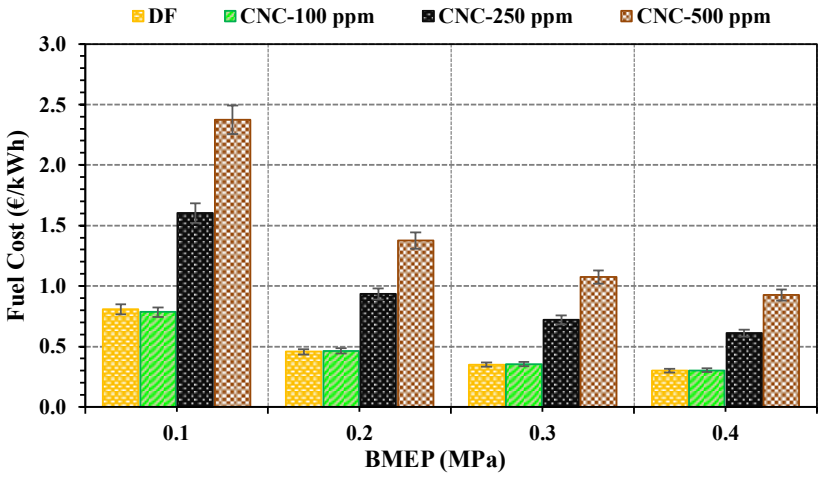

Figure 14. Fuel cost for test fuels across various loadings

To enhance the study's scientific credibility and benchmark CNC performance against metallic nanoparticles, Table 4 was presented. This table provides a comparative overview of key engine performance and emission parameters observed in this study, alongside those reported in previous research on metallic nanoparticle fuel additives. As summarized in Table 4, metallic nanoparticles have been extensively investigated and are known to enhance combustion efficiency, boost engine performance, and reduce emissions. CNCs also yielded similar improvements, albeit to a different extent. These variations can also arise due to differences in experimental setups, fuel types, testing methodologies, nanoparticle sizes and concentrations, and environmental conditions. Therefore, comprehensive engine tests should be conducted under identical conditions, using the same equipment and nanoparticle concentrations to enable a meaningful comparison between CNC and metallic nanoparticles. Although this lies beyond the scope of the present study due to the time and effort required, it is recommended for future research. Overall, CNC performance is comparable to or slightly less than that of its metallic counterparts; however, it presents lower environmental and health risks due to its renewable and biodegradable characteristics. Additionally, it is safe and compatible with both conventional fuels and biofuels.

Table 4. Summary of key findings from this study and previous research on metallic nanoparticles

Reference	NP Type	NP concentration	Engine type	Fuel	Combustion	Performance	Emissions
This study	CNC	100, 250, and 500 ppm	DI, 4-stroke, diesel engine	DF	NHRR 2.97%↑	BSFC 3.95% ↓ and BTE 2.73% ↑	NO_X 7.99%↓, CO_2 2.63%↑, smoke 13.60% ↓
Ref. [26]	TiO_2	200 mg/L	DI, 4-stroke, diesel engine	B20	CP↑, ID 24.73%↓	BTE 6.69%↑	CO 46.54%↓, HC 28.40%↓, NOx 2.30% ↓
Ref. [27]	CeO_2	25, 50, 75, and 100 ppm	DI, 4-stroke, diesel engine	DF	CP 3.75%↑, ID 2.77%↓	BTE 13.73%↑, BSFC 12.08% ↓	NO_X 7.56%↑, CO 13.26%↓, HC 15.49%↓, smoke 17.64%↓
Ref. [28]	CuO	25, 50, and 75 ppm.	DI, 4-stroke, diesel engine	B20	NHRR 5.44%↑	BTE 4.94%↑, BSFC 13.17% ↓	NO_X 1.8%↑, CO_2 5.16%↑, HC 7.45%↓, smoke 8.15%↓
Ref. [29]	Al_2O_3	10, 20, 30, and 40 ppm	DI, 4-stroke, diesel dual-fuel engine	B100	CP ↑, NHRR ↑	BTE 11.5%↑, BSFC 13.17% ↓	NO_X 36.8%↑, CO 11.6%↓, smoke 23.2%↓
Ref. [30]	Al_2O_3, Fe_2O_3	30, 60, and 90 ppm	DI, 4-stroke, air-cooled, diesel engine	DF	CP 4% ↑, NHRR 15% ↑	bp 7.40%↑ BTE 14%↑, BSFC 9% ↓	NO_X 23.9%↓, SO_2 23.4%↓, smoke −
Ref. [31]	Al_2O_3, bN	250, and 500 ppm	DI, 4-stroke, diesel engine	DF	CP →, NHRR →, ID %↓	BSFC 9.72% ↓ BTE 6.64%↑,	NO_X 25.85%↓, CO 21.87%↓, HC 9.56%↓
Ref. [32]	Ag_2O, TiO_2	30 and 75 ppm	DI, 4-stroke, diesel engine, 3-cylinder	B100	CP−, NHRR −	BSFC 6.5% ↓ BTE 6.2%↑,	NO_X 16%↑, CO 24%↓, smoke 39.1%↓
Ref. [33]	ZnO	50 ppm	DI, 4-stroke, air-cooled, diesel engine	B20	CP ↑, NHRR ↑	bp 3.7%↑ BTE 4.34%↑, BSFC 6.44% ↓	NO_X − , CO− , smoke −
Ref. [34]	MgO	100 and 200 ppm	Single-cylinder diesel engine	B20	CP 1.67% ↑, NHRR 1.82% ↑, RPR ↑	BTE −, BSFC −	NO_X 2.21%↑, CO 10.23%↓, HC 17.18%↓, smoke −

Symbols: ↑: increase, ↓: decrease, →: no or slight change, −: data is not available

Abbreviations: Al_2O_3: Alumina Oxide, Ag_2O: silver oxide, bN: Boron nitride, B20: 80% diesel + 20%biodiesel, B100: 100% biodiesel, BSFC: brake-specific fuel consumption, BTE: brake-thermal efficiency, bp: brake power, bN: boron nitride, CNC: crystalline nanocellulose, CuO: Copper oxide, CeO_2: Cerium oxide, CP: cylinder pressure, DF: diesel fuel, DI: direct injection, Fe_2O_3: Iron oxide, ID: ignition delay, MgO: Magnesium oxide, NP: nanoparticle, RPR: rate of pressure rise, ZnO: Zinc oxide.

4. CONCLUSIONS

This experimental study aims to investigate CNC as a potential alternative to conventional metallic nanofuel additives and presents preliminary findings not previously reported. Commercially available CNC was dispersed in standard diesel fuel at 100 ppm, 250 ppm, and 500 ppm, and evaluated using fuel specifications and engine tests. The addition of CNC to diesel fuel increased the fuel's density, flash point, and distillation temperatures. However, it did not affect the CFPP temperature, even at concentrations up to 500 ppm. CNC improved in-cylinder combustion and increased the heat release rate. CNC improved engine performance, with the 500 ppm CNC concentration producing the lowest BSFC and highest BTE. NOx emissions and smoke opacity were reduced with CNC-added fuels. However, CNC showed a greater reduction in NOx emissions at lower concentrations than at higher ones. Due to improved combustion, CNC-added fuels produced higher CO_2 emissions compared to diesel fuel. The fuel cost analysis indicated that only CNC at 100 ppm is cost-effective and viable, as its fuel cost is comparable to diesel. The initial findings indicate that CNC has potential as a nanofuel additive in diesel fuel and could be a viable alternative to traditional metal-based nanofuel additives. However, further research is needed to fully assess CNC as an engine fuel additive. Future studies should compare its performance directly with that of conventional metallic nanofuel additives.

ACKNOWLEDGEMENTS

The authors would like to acknowledge the Scientific and Technological Research Council of Türkiye (TÜBİTAK).

FUNDING

TÜBİTAK 2209-A University Student Research Projects Support Program funded this study.

CONFLICT OF INTEREST

The authors declare no conflicts of interest.

AUTHORS CONTRIBUTION

K. Keskin (Funding acquisition; Project administration; Investigation)

A. Çakmak (Methodology; Investigation; Data curation; Writing - original draft; Resources; Supervision)

REFERENCES

[1] A. Çakmak, "Improvement of exhaust emissions in a diesel engine with the addition of an oxygenated additive to diesel-biodiesel blends," *Energetika*, vol. 68, no. 1, pp. 79–90, 2022.

[2] C. Grütering, C. Honecker, M. Hofmeister, M. Neumann, L. Raßpe-Lange, M. Du, et al., "Methyl ketones: a comprehensive study of a novel biofuel," *Sustainable Energy & Fuels*, vol. 8, no. 9, pp. 2059–2072, 2024.

[3] R. D. Reitz, H. Ogawa, R. Payri, T. Fansler, S. Kokjohn, Y. Moriyoshi, et al., "IJER editorial: The future of the internal combustion engine," *International Journal of Engine Research*, vol. 21, no. 1, pp. 3–10, 2020.

[4] A. M. Khedr, M. El-Adawy, M. A. Ismael, A. Qador, A. Abdelhafez, R. Ben-Mansour, et al., "Recent fuel-based advancements of internal combustion engines: Status and perspectives," *Energy & Fuels*, vol. 39, no. 11, pp. 5099–5132, 2025.

[5] M. A. I. Malik, M. A. Kalam, M. M. Abbas, A. S. Silitonga, and A. Ikram, "Recent advancements, applications, and technical challenges in fuel additives-assisted engine operations," *Energy Conversion and Management*, vol. 313, p. 118643, 2024.

[6] M. Ali Ijaz Malik, M. A. Kalam, M. Mujtaba Abbas, A. Susan Silitonga, and A. Ikram, "Recent advancements, applications, and technical challenges in fuel additives-assisted engine operations," *Energy Conversion and Management*, vol. 313, p. 118643, 2024.

[7] P. Vignesh, V. Jayaseelan, P. Pugazhendiran, M. S. Prakash, and K. Sudhakar, "Nature-inspired nano-additives for Biofuel application – A review," *Chemical Engineering Journal Advances*, vol. 12, p. 100360, 2022.

[8] Y. Singh, H. S. Pali, N. K. Singh, A. Sharma, and A. Singla, "Effect of nanoparticles as additives to the biofuels and their feasibility assessment on the engine performance and emission analysis—A review," *Proceedings of the Institution of Mechanical Engineers, Part E: Journal of Process Mechanical Engineering*, vol. 237, no. 2, pp. 492–510, 2022.

[9] M. S. Mujaheed Khan, P. Kumar, I. Ansari, and N. Sahoo, "Experimental analysis of diesel engine characteristics powered with Al2O3 doped mesua ferrea linn vegetable oil-diesel blend," *Fuel*, vol. 381, p. 133251, 2025.

[10] J. N. Nair, T. Nagadurga, V. D. Raju, H. Venu, S. Algburi, S. Kamangar, et al., "Impact of fuel additives on the performance, combustion and emission characteristics of diesel engine charged by waste plastic bio-diesel," *Case Studies in Thermal Engineering*, vol. 67, p. 105755, 2025.

[11] E. Çılğın, "Validation of magnesium oxide additive effects on diesel engine performance through crystal structure and thermal stability analyses," *Heat Transfer*, vol. 54, no. 2, pp. 1665–1680, 2025.

[12] T. Sathish, J. Giri, R. Saravanan, R. Zairov, and S. M. M. Hasnain, "Nano-fuels of Al2O3/SiO2/MgO/tamarind seed oil biodiesel for CI engines: An evaluation of combustion consumption and emission performance," *International Journal of Thermofluids*, vol. 23, p. 100815, 2024.

[13] M. S. Almanzalawy, M. F. Elkady, A. Sanad, M. Yousef, and A. E. Elwardany, "Combined effects of ferric oxide nanoparticles and C2–C4 alcohols with diesel/biodiesel blend on diesel engine operating characteristics," *Alexandria Engineering Journal*, vol. 103, pp. 38–50, 2024.

[14] B. Doğan, M. K. Yeşilyurt, H. Yaman, N. Korkmaz, and A. Arslan, "Green synthesis of SiO_2 and TiO_2 nanoparticles using safflower (Carthamus tinctorius L.) leaves and investigation of their usability as alternative fuel additives for diesel-safflower oil biodiesel blends," *Fuel*, vol. 367, p. 131498, 2024.

[15] J. D. Ampah, A. A. Yusuf, E. B. Agyekum, S. Afrane, C. Jin, H. Liu, et al., "Progress and recent trends in the application of nanoparticles as low carbon fuel additives—A state of the art review," *Nanomaterials*, vol. 12, no. 9, p. 1515, 2022.

[16] A. B. Sengul and E. Asmatulu, "Toxicity of metal and metal oxide nanoparticles: a review," *Environmental Chemistry Letters*, vol. 18, no. 5, pp. 1659–1683, 2020.

[17] E. Matei, M. Râpă, I. M. Mateş, A. F. Popescu, A. Bădiceanu, A. I. Balint, et al., "Heavy metals in particulate matter—Trends and impacts on environment," *Molecules*, vol. 30, no. 7, p. 1455, 2025.

[18] N. Yıldırım, "Nanotechnology and the futurist green polymer, nanocellulose," *Turkish Journal of Forestry Research*, vol. 5, no. 2, pp. 185–195, 2018.

[19] M. S. Newaz Kazi, K. Shaikh, W. A. Khan, and M. N. Mohd Zubir, "Nanocellulose: Fundamentals and Applications," M. S. N. Kazi, Ed., Rijeka: IntechOpen, 2024.

[20] Nanografi, "Nanocrystalline Cellulose," [Online] Available: https://shop.nanografi.com/popular-products/cellulose-nanocrystal-nanocrystalline-cellulose-cnc/

[21] J. P. Holman, *Experimental Methods for Engineers*, 7th ed. New York: McGraw-Hill Series in Mechanical Engineering, 2001.

[22] S. Gumus, H. Ozcan, M. Ozbey, and B. Topaloglu, "Aluminum oxide and copper oxide nanodiesel fuel properties and usage in a compression ignition engine," *Fuel*, vol. 163, pp. 80–87, 2016.

[23] M. P, P. P, and R. Sathyamurthy, "Analysis on performance and emission characteristics of corn oil methyl ester blended with diesel and cerium oxide nanoparticle," *Case Stud. Therm. Eng.*, vol. 26, p. 101077, 2021.

[24] Ü. Ağbulut, C. Uysal, E. J. C. Cavalcanti, M. Carvalho, M. Karagöz, and S. Saridemir, "Exergy, exergoeconomic, life cycle, and exergoenvironmental assessments for an engine fueled by diesel–ethanol blends with aluminum oxide and titanium dioxide additive nanoparticles," *Fuel*, vol. 320, p. 123861, 2022.

[25] A. Çakmak, "Comparative research on acetone-butanol-ethanol (ABE) and butanol (Bu) as next-generation biofuels in compression ignition engine," *Thermal Science and Engineering Progress*, vol. 55, p. 102956, 2024.

[26] C. Jit Sarma, P. Sharma, B. J. Bora, D. K. Bora, N. Senthilkumar, et al., "Improving the combustion and emission performance of a diesel engine powered with mahua biodiesel and TiO_2 nanoparticles additive," *Alexandria Engineering*, vol. 72, pp. 387–398, 2023.

[27] M. Celik and S. and Uslu, "Experimental investigation of diesel engine running on diesel fuel supplemented with CeO2 metal nanoparticles," *Energy Sources, Part A: Recovery, Utilization, and Environmental Effects*, vol. 45, no. 1, pp. 246–262, 2023.

[28] P. M. Rastogi, A. Sharma, and N. Kumar, "Effect of CuO nanoparticles concentration on the performance and emission characteristics of the diesel engine running on jojoba (Simmondsia Chinensis) biodiesel," *Fuel*, vol. 286, p. 119358, 2021.

[29] K. A. Sateesh, V. S. Yaliwal, M. E. M. Soudagar, N. R. Banapurmath, H. Fayaz, M. R. Safaei, et al., "Utilization of biodiesel/Al2O3 nanoparticles for combustion behavior enhancement of a diesel engine operated on dual fuel mode," *Journal of Thermal Analysis and Calorimetry*, vol. 147, no. 10, pp. 5897–5911, 2022.

[30] M. Nouri, A. H. M. Isfahani, and A. Shirneshan, "Effects of Fe2O3 and Al2O3 nanoparticle-diesel fuel blends on the combustion, performance and emission characteristics of a diesel engine," *Clean Technologies and Environmental Policy*, vol. 23, no. 8, pp. 2265–2284, 2021.

[31] Ü. Ağbulut and S. Sarıdemir, "Synergistic effects of hybrid nanoparticles along with conventional fuel on engine performance, combustion, and environmental characteristics," *Energy*, vol. 292, p. 130267, 2024.

[32] M. Çelik, M. Mehregan, C. Bayındırlı, and M. Moghiman, "Optimization analysis of a compression ignition engine running with silver oxide and titanium dioxide nanoparticles blended into canola biodiesel and pure diesel using Taguchi technique," *Journal of Chemical and Petroleum Engineering*, vol. 59, no. 1, pp. 65-80, 2025.

[33] M. El-Adawy, "Effects of diesel-biodiesel fuel blends doped with zinc oxide nanoparticles on performance and combustion attributes of a diesel engine," *Alexandria Engineering Journal*, vol. 80, pp. 269–281, 2023.

[34] H. Deviren, Ç. Erdal, and S. Aydin, "Study on using nano magnesium oxide (MNMgO) nanoparticles as fuel additives in terebinth oil biodiesel blends in a research diesel engine," *Energy Sources, Part A: Recovery, Utilization, and Environmental Effects*, vol. 45, no. 4, pp. 12181–12200, 2023.